Slovak University of Technology in Bratislava
Institute of Information Engineering, Automation, and Mathematics

PROCEEDINGS

of the 18th International Conference on Process Control

Hotel Titris, Tatranská Lomnica, Slovakia, June 14 – 17, 2011

ISBN 978-80-227-3517-9

http://www.kirp.chtf.stuba.sk/pc11

Editors: M. Fikar and M. Kvasnica

Petrová, J., Mudrová, M., Procházka, A., Fojt, J.: Application of Mathematical Morphology on Nanostructure Image Processing, Editors: Fikar, M., Kvasnica, M., In *Proceedings of the 18th International Conference on Process Control*, Tatranská Lomnica, Slovakia, 273–277, 2011.

Full paper online: http://www.kirp.chtf.stuba.sk/pc11/data/abstracts/049.html

APPLICATION OF MATHEMATICAL MORPHOLOGY ON NANOSTRUCTURE IMAGE PROCESSING

J. Petrová * **M. Mudrová** * **A. Procházka** * **J. Fojt** **

* *Department of Computing and Control Engineering, ICT Prague, Technická 5, 166 28 Praha 6*
fax : +420 220 445 053 and e-mail : petrovaj@vscht.cz
** *Department of Metals and Corrosion Engineering, ICT Prague, Technická 5, 166 28 Praha 6*
fax : +420 220 444 400 and e-mail : fojtj@vscht.cz

Abstract: Mathematical morphology is a very effective tool on image segmentation. This paper presents selected methods of mathematical morphology that are applied to the microscopic images of nanomaterials. The first part briefly describes the mathematical background of the fundamental morphological methods, including their application on the test image. The second part contains an application both of binary and grayscale morphological methods on the nanostructure images. The influence of various structure elements is investigated, as well.

Keywords: binary morphology, nanostructure image processing, grayscale morphology

1. INTRODUCTION

Image processing is applied as an effective tool for various image analysis in many branches of science, Kuehn (1998), Wu (1995), Sorzanoa (2004). Presented paper is focused on analysis of nanomaterial images.

These nanomaterial seems to be one of the options of surface bioactivation of titanium implants that are used in medicine, Fojt (2010). Nanomaterial properties assessment is one of the essential issues in the process of material development while the tube diameter should be evaluated as well as a side thickness and other quantities. The material properties quantities could be based on the processing of microscopic images, Hodneland (2006), Bunes (2008), Kiang (1998), Gommes (2003).

A lot of various methods are used for segmentation and analysis of given microscopy images, such as a low-pass filtering, application of watershed transform, adaptive thresholding, mathematical morphology Dougherty (2003), Heijmans (1998), Horgan (1998), convex hull and others.

Methods of mathematical morphology could be used for processing both of binary and grayscale images, Gonzalez (2002), Hlavac (2002), Hanbury (2001). This paper looks out only a part of the complex algorithm of given data processing that concerns of an application of binary mathematical morphology methods.

2. MATHEMATICAL BACKGROUND

Mathematical morphology provides a tool for extraction of those image components that are useful in the representation and description of a region shape. The most common use of mathematical morphology is in image enhancement, segmentation and restoration, edge detection, texture and component analysis, curve filling, noise reduction etc. A grayscale digital image generally can be represented as a set of elements, values of which are vectors of the 3–D integer space Z^3. The first two components represent coordinates (x, y) of the pixel and the third one its discrete graylevel value. A binary image A can be considered as a set of n white pixels $A = \{(x_1, y_1), (x_2, y_2), \ldots, (x_n, y_n)\}$ where vector $\{(x_i, y_i) \in Z^2\}$ corresponds to pixel coordinates.

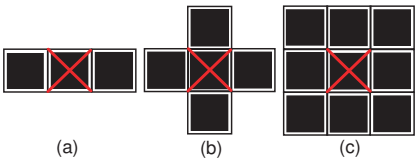

Figure 1. Examples of common structural elements:
(a) $B1 = \{(-1,0),(0,0),(1,0)\}$,
(b) $B2 = \{(-1,0),(0,-1),(0,0),(1,0),(0,1)\}$,
(c) $B3 = \{(-1,0),(0,-1),(0,0),(1,0),(0,1),(1,1),(1,-1),(-1,-1),(-1,1)\}$

Morphological operators are given by the relationships between a set of points of an original image A and another point set, which is called a structural element B. Various types of structural elements can be used. Examples of the most common structural elements are presented in Fig. 1.

Dilation, erosion, opening and closing are the basic morphological transformations.

2.1 Binary Morphology

Morphological operations can be defined with Minkowski operators, other description can be used, as well, Gonzalez (2002), Farouki (2001).

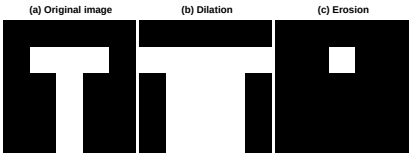

Figure 2. (a) Original image (point set A), (b) Dilation of A by structure element $B1$, (c) Erosion of A by $B1$

A *Dilation* operator of A by B, denoted $A \oplus B$ is defined as

$$A \oplus B = \{z \mid (\hat{B})_z \cap A \neq \emptyset\} \tag{1}$$

where A is a set of points of the original image and set B is a selected structural element. $\hat{B}$ means a reflection of the set B. Dilation of A by B is the set of all displacements, z, such that $\hat{B}$ and A overlap by at least one element. A gaps bridging is one of common applications of dilation. Dilation with a suitable structural element use makes objects larger and so that it fills gaps in an image.

An *Erosion* operator of A by B, denoted $A \ominus B$ is defined as

$$A \ominus B = \{z \mid (B)_z \subseteq A\} \tag{2}$$

where A is a set of points of an original image and a set B is a structural element, again. Erosion of A by B is the set of all points z such that B, translated by z, is contained in A.

The simplest application of erosion is an elimination of small details in an image. Objects smaller than a structural element are removed. This property forms a base for a morphological operations. Example of a simple effect of dilation and erosion on the test image is presented in Fig. 2. The structural element $B1$ is used for test. Dilation expands objects and erosion shrinks them. A combination both of them changes the image but saves object size.

Opening of an image set point A with a structural element B, denoted $A \circ B$, is defined as an erosion followed by a dilation with the same structural element use

$$A \circ B = (A \ominus B) \oplus B. \tag{3}$$

Closing A with B, denoted $A \bullet B$, is defined as a dilation followed by an erosion

$$A \bullet B = (A \oplus B) \ominus B. \tag{4}$$

Both of these operations smooth the object contours. Opening separates objects connected with narrow isthmuses, closing eliminates small gaps and gets through narrow breaks. An example of simple effect of opening and closing is presented in Fig. 3. The same structural element as in the Fig. 2 has been used.

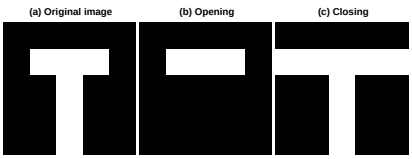

Figure 3. (a) Original image (point set A), (b) Opening A by structure element $B1$, (c) Closing A by $B1$

2.2 Grayscale Morphology

Basic binary morphological operation can be extended to grayscale images, Gonzalez (2002), Hanbury (2001). Operations deal with the input image function $f(x, y)$ and a structural element $b(x, y)$.

Grayscale dilation of f by b, $f \oplus b$, is defined as

$$(f \oplus b)(s,t) = max\{f(s-x, t-y) + b(x, y) \mid \\ \mid (s-x), (t-y) \in D_f; (x, y) \in D_b\} \tag{5}$$

where D_f and D_b are the domains of f and b.

After application of dilation on a grayscale image, output image is brighter than an input one if all the values of the structural element are positive. Dark details are reduced or eliminated.

Grayscale erosion is based on the minimum value of $(f - b)$ choosing in the interval defined by structural element b. The Erosion of f by b, $f \ominus b$, is defined as

$$(f \ominus b)(s,t) = min\{f(s+x, t+y) - b(x, y) \mid \\ \mid (s+x), (t+y) \in D_f; (x, y) \in D_b\} \tag{6}$$

where D_f and D_b are the domains of f and b.

Output image after grayscale erosion application is darker than input one if all elements of the structural element are positive. The bright details that are smaller than the structural element are reduced.

Grayscale opening and closing have the same form as their binary alternates. The opening of grayscale image f by the structural element b, $f \circ b$, is defined as

$$f \circ b = (f \ominus b) \oplus b \tag{7}$$

The grayscale closing of f by b, $f \circ b$, is defined as

$$f \bullet b = (f \oplus b) \ominus b \tag{8}$$

Top-hat transformation h of an image f is defined as

$$h = f - (f \circ b) \tag{9}$$

where f is an original image and b is a structural element. This transformation is useful for enhancing detail in background.

Morphological gradient, denoted g, highlight sharp grey-level transitions in the input image. It is defined as

$$g = (f \oplus b) - (f \ominus b) \tag{10}$$

3. NANOSTRUCTURE IMAGE PROCESSING

Nanostructure image processing features a very important part of classification process of nanomaterials quality. There is presented a selected cut of image of titanium dioxide tubes, Fojt (2010), in Fig. 4a. One of the important factor representing the material quality is an inner tube diameter. Methods of image processing seems to be a suitable tool to obtain the desired value. The essential step of the nanomaterial image processing is a separation of the inner area of tubes from the background. Preprocessing of these images based on digital filters application is

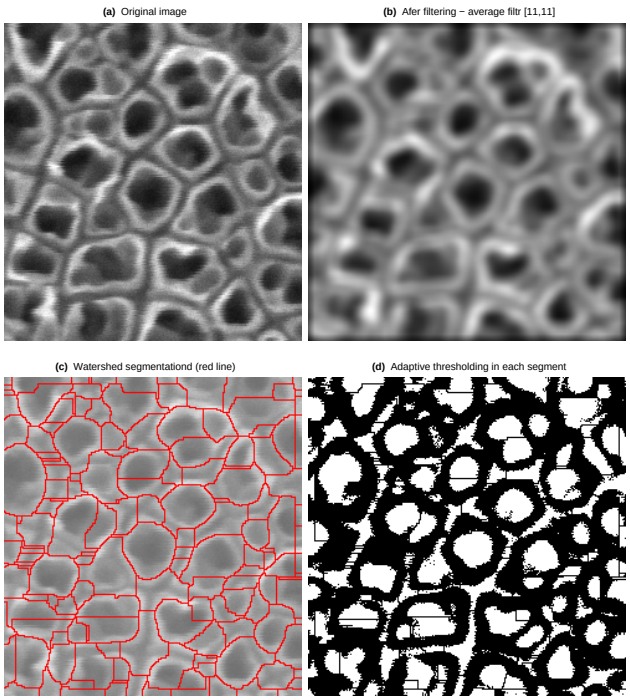

Figure 4. Image preprocessing before morphology use: (a) An original image, (b) Lowpass filter application, (c) Watershed segmentation, (d) Adaptive thresholding result

necessary, as well. The filter size and cutoff frequency of lowpass filter used dependent on image character. The filtration reduces a level of noise in the image and it improves results of segmentation in the following step, Fig. 4b.

In the next step the image is divided into segments by means of watershed transform Eq. (10), Fig. 4c. After that, an adaptive thresholding is performed inside of each segment. Adaptive thresholding is used because of very different grayscale level in each part of the image. Setting of one thresholding value for whole the image is unsuitable in this case. Although the adaptive thresholding application provides satisfying results, there are still undesired artifacts in the resulting image, Fig. 4d. Some of them

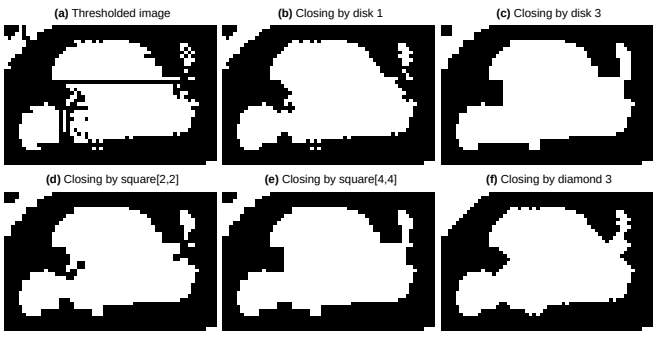

Figure 5. Selected results of closing operation by means of various types of structural element in zoomed cut of an image: (a) Part of thresholded image, (b) Closing by disk size 1, (b) Closing by disk size 3, (d) Closing by square size [2,2], (e) Closing by square size [4,4], (f) Closing by diamond size 3

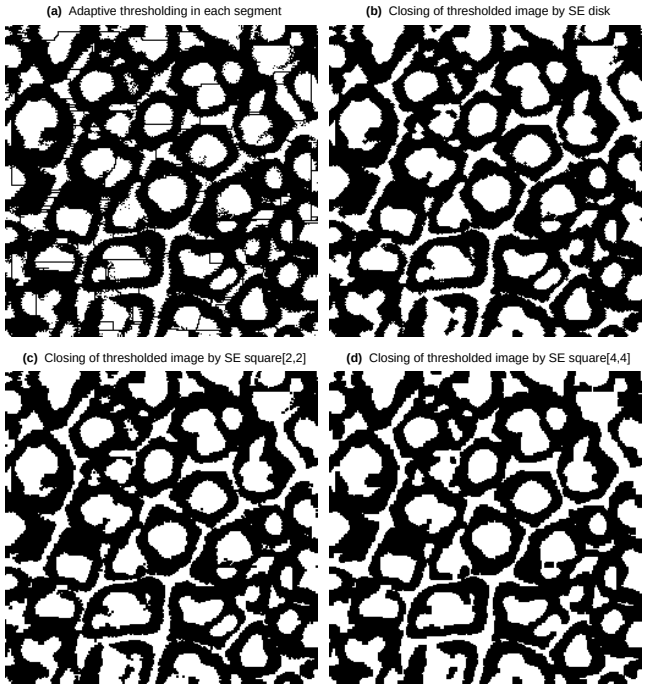

Figure 6. Closing of thresholded image cut by various structural element: (a) Thresholded image, (b) Closing by disk 1, (b) Closing by structural element type disk size 1, (c) Closing by structural element type square size [2,2], (d) Closing by structural element type square size [4,4]

imply from the inner area selection only, without segments border. Application of mathematical morphology seems

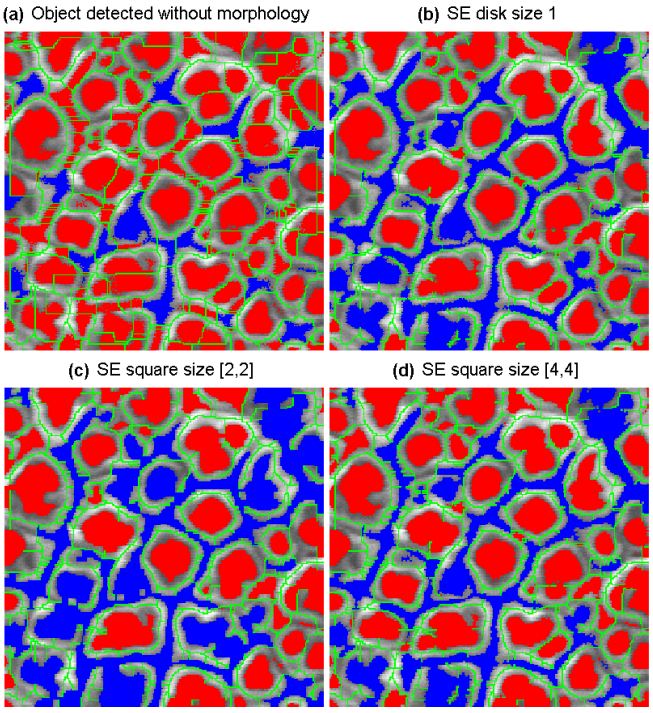

Figure 7. Convex area (red) and non-convex area (blue) detected by various SE: (a) without morphology, (b) SE disk size 1, (c) SE square size [2,2], (d) SE square size [4,4]

to be an effectual tool for elimination of these undesired effects, Fig. 6. Closing operation can remove small holes inside the objects and it smooths out the objects contours. The result of this operation depends on the shape of structural element used, of course. Various structural elements B were tested on the real image set. A selected zoom cut processed by mean of various structural element is presented in Fig 5. Only the symmetric structural elements have been considered, as it is possible to suppose an isotropic material properties.

As the tubes are supposed to have a convex crosscut, non-convex areas are excluded from the next processing and the area of convex segment is considered only, Fig. 7.

Results obtained with the application of various SE are presented in Tab. 1. Sample of selected structural element is Disk1=$\{(-1,0),(0,-1),(0,0),(1,0),(0,1)\}$ or Square[2,2]=$\{(0,0),(0,1),(1,0),(1,1)\}$.

The application of mathematical morphology methods implicates reduction of a number of objects found in the image, see Tab. 1. Results obtained by application of various structural elements are comparable. It's not possible to appoint the best structural element explicitly. The elements in form of disk and square seems to be useful for this type of images.

Table 1. Results obtained with various structural elements use

Structural Element	The Number of Tubes	Tube Area Percentage of the Image	Average Tube Area (px)	Standard Deviation
–	248	32,21	85,11	147,33
disk 1	100	27,95	183,16	254,08
disk 3	50	21,27	278,84	304,34
square [2,2]	83	27,49	217,06	262,94
square [4,4]	58	25,52	288,34	294,39
diamond 3	61	21,51	231,13	293,58

4. CONCLUSION

Nanostructure image processing is a very important part of classification process of nanomaterials quality. Application of mathematical morphology methods can improve object detection in these images. The best structural element for this detection cannot be exactly defined, as the image resolution seems to be a basic factor for structural element size and shape selection, too. Obtained results depend on an original image quality, as well. Based on testing, structural element in the form disk and square seems to suitable for processing of the given images.

Used images originate from electron microscope TESCAN VEGA 3 SBU. The algorithm was developed in MATLAB environment, ver. 2010a, and it was tested on computer with following parameters: processor Intel(R) Core(T2) 2CPU, 2,40 GHz, RAM 4GB, OS Win7 32bit.

Application of various type of a structural element has similar demands concerning a runtime. There is a comparison of runtime values for selected structural elements use, Tab. 2.

Table 2. Runtime obtained with an application of various structural elements

	Disk 1	Disk 3	Square[2,2]	Square[4,4]	Diamond3
Runtime[s]	0,118	0,234	0,031	0,027	0,066

ACKNOWLEDGMENTS

This work has been supported by the Ministry of Education of the Czech Republic (programs No. MSM 6046137306 and MSM 6046137302). Financial support from specific university research (MSMT No 21/2011) is acknowledged, as well.

REFERENCES

Gonzalez R.C. and Woods R.E. *Digital Image Processing.* Prentice Hall, Upper Saddle River, New Jersey 07458, 2002.

Dougherty E.R. and Lotufo R.A. *Hands-on Morphological Image Processing.* SPIE, Bellingham, Washington 98227-0010 USA, 2003.

Fojt J., Moravec H. and Joska L. Nanostrukturování slitiny titan-hliník-vanad. *Koroze a ochrana materiálů*, 2010,volume 54 (4), pages 154–154.

Heijmans H.J.A.M. and Roerdink J.B.T.M. *Mathematical Morphology and its Applications to Image and Signal Processing.* Kluwer Academic Publisher, P.O.Box 17, 3300 AA Dordrecht, The Netherlands, 1998.

Hlaváč V. and Sedláček M. *Zpracování signalů a obrazů.* Vydavatelství ČVUT, Praha, 2000.

Wu K., Gauthier D. and Levine M.D. Live Cell Image Segmentation. *IEEE Transactions on Biomedical Engineering*, Jan. 1995,volume 4, No. 1.

Kuehn M.,Hausner M., Bungartz H.-J., Wagner M.,Wilderer P.A. and Wuertz S. Automated Confocal Laser Scanning Microscopy and Semiautomated Image Processing for Analysis of Biofilms. *Applied and Enviromental Microbiology*, Nov. 1998, volume 64, No. 11.

Sorzanoa C.O.S., Marabinia R., Velazquez-Muriela J., Bilbao-Castroa J.R., Scheresa S.H.W., Carazoa J.M. and Pascual-Montanoa A. XMIPP: a new generation of an open-source image processing package for electron microscopy. *Journal od Structural Biology*, 2004, vol. 148, pages 194–204.

Hodneland E., Lundervold A., Gurke S., Tai X.-Ch., Rustom A. and Gerdes H.-H. Automated Detection of Tunneling Nanotubes in 3D Images. *International Society for Analytical Cytology*, 2006.

Farouki R.T., Moon H.P. and Ravani B. Minkowaki Geometric Algebra of Complex Sets. *Geometriae Dedicata*, 2001, vol. 85, pages 283–315.

Horgan G.W. Mathematical Morphology for Analysing Soil Structure Images. *European Journal of Soil Science*, June 1998, vol. 49, pages 161–173.

Hanbury A.G. and Serra J. Morphological Operators on the Unit Circle. *IEEE Transactions on Biomedical Engineering*, Dec. 2001, vol. 10, No. 12.

Bunes B.R., Catravas P.E. and Hagerman, M.E. Image Processing Algorithm for Analyzing Chirality in Carbon Nanotubes. 8th IEEE Conference on Nanotechnology, 2008.

Kiang C.-H., Endo M., Ajayan P.M., Dresselhaus G. and Dresselhaus M.S. Size Effects in Carbon Nanotubes. *Phys. Rev. Lett.*, 1998, vol. 81, pages 1869–1872.

Gommes C., Blacher S., Masenelli-Varlot K., Bossuot Ch., McRae E., Fonseca A., Nagy J.-B., Pirard J.-P. Image analysis characterization of multi-walled carbon nanotubes. *Carbon*, 2003, vol. 41, pages 2561–2572.